CDF/ANAL/TOP/CDFR/7108
Version 1.1
July 29, 2004

Measurement of $B(t \to Wb)/B(t \to Wq)$ in Dilepton and Lepton-Plus-Jets Samples

Ken Bloom, Phillip Killewald, Stephen Miller, Monica Tecchio
University of Michigan

Michael Gold, Dmitri Smirnov, John Strologas
University of New Mexico

Charles Plager
University of California, Los Angeles

Abstract

We measure the ratio of branching fractions $R \equiv B(t \to Wb)/B(t \to Wq)$ by comparing the rates of non-, single- and double-tagged $t\bar{t}$ in 161 pb^{-1} of $p\bar{p}$ collision data. This measurement combines information from three individual measurements that are made in the dilepton and lepton-plus-jets samples. Assuming the nominal value of the b-tagging efficiency, we find $R = 1.11^{+0.21}_{-0.19}$, consistent with the standard-model expectation. Assuming $R = 1$, we find $\epsilon_b = 0.49^{+0.09}_{-0.08}$. Using the Feldman-Cousins technique, we set the limit $R > 0.62$ at 95% CL.

1 Introduction

The branching fraction $R \equiv B(t \to Wb)/B(t \to Wq)$ can be estimated from the relative rates of b tags in identified $t\bar{t}$ events. [1] Such a measurement is independent of any measurement of the overall $t\bar{t}$ production rate, and is also independent of the decay mode of the W. CDF has now performed three measurements of R in Run 2. One uses the sample of lepton-plus-jets events with b tags, and uses "Method 2" to estimate the background levels [1]. This gives a precise estimate of the backgrounds, but because Method 2 does not give a background rate for untagged events, not all possible information for R can be used. Another measurement works with the same lepton-plus-jets sample, but statistically separates signal and background events on the basis of their differing kinematics through a neural-net discriminator [2]. Now the 0-tag sample can be used, but background estimates in the 1-tag and 2-tag sample are not as good as those in the Method 2 analysis. (Both of these analyses are performed on the same data sample, so their results are highly correlated.) Finally, a third analysis measures R in the dilepton sample [3]. Here, all three subsamples can be used, and the backgrounds are measured fairly well, but this is a much smaller $t\bar{t}$ sample than the lepton-plus-jets sample.

In this note, we produce a combined result for the three analyses. We do so by choosing the best available information from each analysis, and putting the information into a joint likelihood function. Given that the inputs have already been determined by the three analyses, the computation of the final result is straightforward.

[1]Some earlier notes have used the variable b instead of R; that notation was admittedly confusing as b is also a quark.

Note	Topic
CDF 6822	Introductory material
CDF 7012	Lepton-plus-jets measurement with Method 2
CDF 7067	Lepton-plus-jets measurement with neural net
CDF 7070	Tagging efficiencies as a function of $R\epsilon_b$
CDF 7100	Dilepton measurement

Table 1: Guide to documentation for the R measurement.

Table 1 gives a list of CDF notes with useful information for the combined result. As this measurement has been explained already in several different places [4], we will skip many details of the methodology. In brief, the product $R\epsilon_b$, where ϵ_b is the single b-jet tagging efficiency, can be determined by any pair of tag rates in $t\bar{t}$ events. This is easily demonstrated if we make the naive assumption that all b-type quarks in a $t\bar{t}$ event are taggable and uncorrelated, and no other quarks can be tagged as b quarks. Then, if each of two top quarks in the event has a probability R to decay to a b quark, and there is an efficiency ϵ_b to tag the quark jet, the efficiencies to detect zero, one or two b jets in the event are

$$\epsilon_0 = (1 - R\epsilon_b)^2, \quad \epsilon_1 = 2R\epsilon_b(1 - R\epsilon_b), \quad \epsilon_2 = (R\epsilon_b)^2, \tag{1}$$

and therefore

$$R\epsilon_b = \frac{2}{\epsilon_1/\epsilon_2 + 2} = \frac{1}{2\epsilon_0/\epsilon_1 + 1} = \frac{1}{\sqrt{\epsilon_0/\epsilon_2} + 1}, \tag{2}$$

or

$$R\epsilon_b = \frac{2}{N_1/N_2 + 2} = \frac{1}{2N_0/N_1 + 1} = \frac{1}{\sqrt{N_0/N_2} + 1}, \tag{3}$$

where N_i are the number of $t\bar{t}$ events observed with i tags. The naive assumptions are not true (and much of the analysis revolves around accounting for that fact), but the equations illustrate the principle of the measurement – any two tagging rates determine $R\epsilon_b$, and three tagging rates overdetermine $R\epsilon_b$. The ratios of tag rates can only determine the product $R\epsilon_b$, as it is impossible to tell the difference between missing tagged jets due to tagging inefficiency ($\epsilon_b < 1$) and missing tagged jets due to the absence of b quarks ($R < 1$). However, $R\epsilon_b$ can be determined independently of the total rate of $t\bar{t}$ production (*i.e.* the cross section), and it can be measured independently of the decay mode of the W boson produced in top decay. In the end, rather than actually computing the ratios, we form a likelihood distribution which compares the observed numbers of tagged events with a predicted rate that is a function of $R\epsilon_b$; the likelihood is maximized with respect to $R\epsilon_b$.

In Section 2, we review the inputs to the three R measurements – in particular, the estimates of background in the various subsamples, and the tagging efficiencies as a function of $R\epsilon_b$. Some of these inputs will also be inputs to the combined measurement; we explain which ones we choose. In Section 3, we describe the likelihood function, and in Section 4 we show our expected sensitivity for the combined measurement. Our results are given in Section 5.

2 Inputs

The R measurement is performed in three disjoint event samples – lepton-plus-jets events with at least four jets (L4J), lepton-plus-jets events with exactly three jets (L3J), and dileptons (LL). In turn, each of those samples are broken down into the numbers of events with zero, one and two

	M2
0-tag	undetermined
1-tag	16.0 ± 2.4
2-tag	0.8 ± 0.2

Table 2: Background estimates in the L3J sample.

	M2	NN
0-tag	undetermined	$62.4^{+8.5}_{-9.3}$
1-tag	4.2 ± 0.7	$5.8^{+5.6}_{-5.2}$
2-tag	0.2 ± 0.1	$0.1^{+0.9}_{-0.0}$

Table 3: Background estimates in the L4J sample.

tags. Thus, for nine different subsamples, we need to estimate the backgrounds to $t\bar{t}$, so we know the true $t\bar{t}$ tag rates.

Tables 2, 3, and 4 give the background estimates for nine subsamples as determined by the different analyses – Method 2 (M2), the neural net (NN) and dilepton (LL). For only two subsamples, the 1-tag and 2-tag L4J, is there more than one analysis providing estimates. In that particular case, M2 gives significantly smaller uncertainties than NN. While we could make an attempt to combine the estimates from the two analyses, it is clear that the M2 results will dominate. Therefore, in computing R, we will use the M2 background estimates for those two samples. We note that some portions of the M2 backgrounds do have a dependence on the b-tagging scale factor must be accounted for when extracting R, and this is done in Section 5. The NN backgrounds do not suffer from this feature.

When we compute the likelihood, we must keep in mind some correlations in these background estimates. The overall normalization of the M2 backgrounds are completely correlated across samples with different numbers of tags and different numbers of jets. The estimates of the distribution of M2 backgrounds across the 1-tag and 2-tag samples are anticorrelated with each other. The background estimates from the NN analysis can be considered completely uncorrelated with those from any of the other analyses. This is also true of the dilepton backgrounds. In that analysis, the 0-tag and 1-tag estimates are anticorrelated.

These background estimates are one set of inputs to the likelihood. The other inputs (besides the number of events observed in the data, of course) are the efficiencies to detect zero, one or two tags in a $t\bar{t}$ event ("event-tagging efficiencies"). These efficiencies depend on the selection cuts, but also on $R\epsilon_b$ itself; the larger the product, the greater the 2-tag efficiency and the lesser the 0-tag efficiency. The efficiencies as a function of $R\epsilon_b$ have been calculated previously [5, 2], and the results are shown in Figures 1 and 2.

Tags in $t\bar{t}$ events mostly arise from b quarks, but they can also come from other sources. In particular, if $R < 1$, then light quarks are produced in top decay instead of b quarks, and the b-tagging efficiency thus becomes $R\epsilon_b + (1 - R)\epsilon_q \equiv R\Delta\epsilon + \epsilon_q$, where ϵ_q is the efficiency to tag a

	LL
0-tag	2.0 ± 0.6
1-tag	0.2 ± 0.1
2-tag	0

Table 4: Background estimates in the dilepton sample.

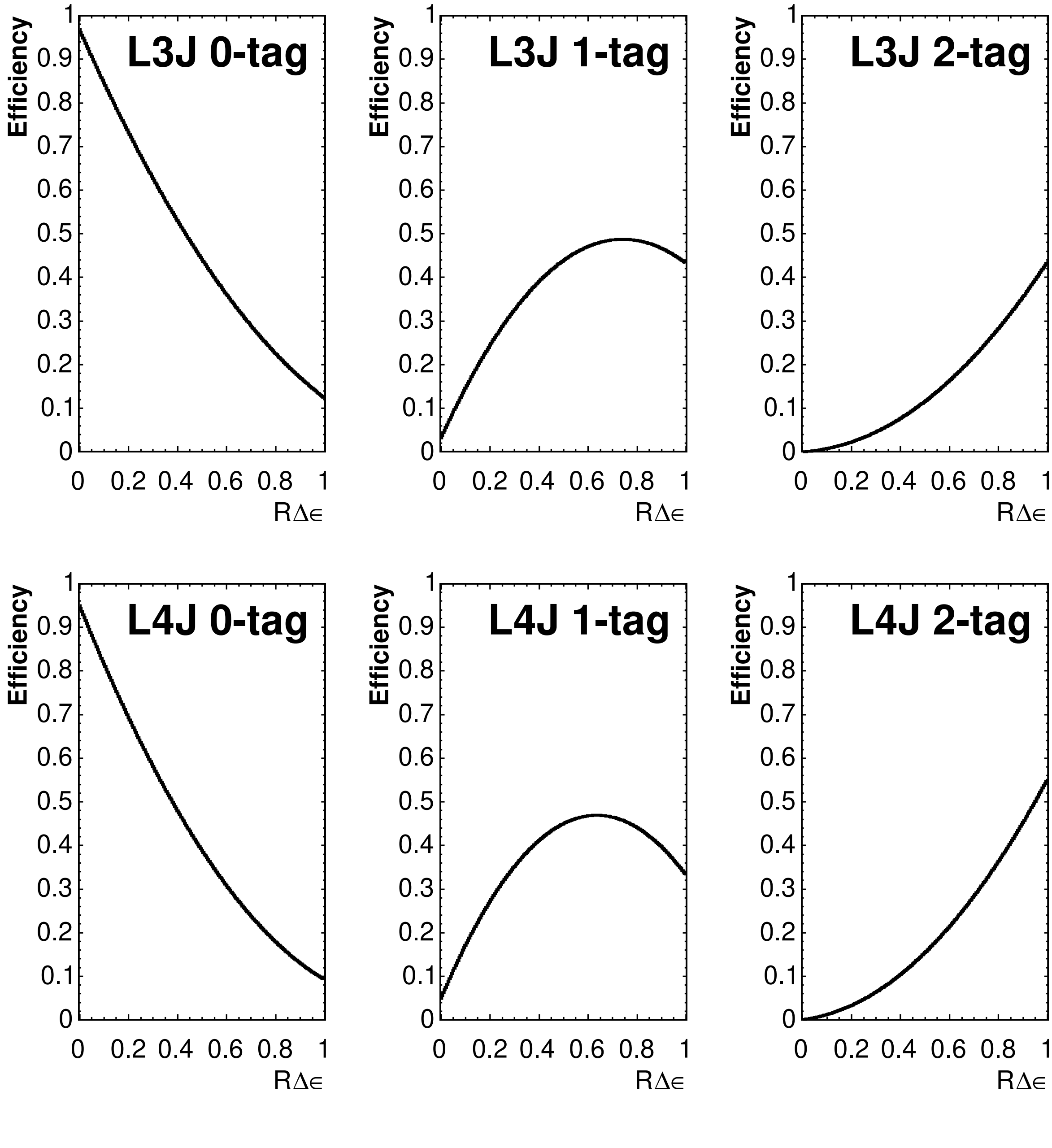

Figure 1: Efficiencies to detect zero (left), one (center) and two (right) tags in lepton plus jets events in the L3J (top) and L4J (bottom) samples. The nominal value of $R\Delta\epsilon$ is 0.436.

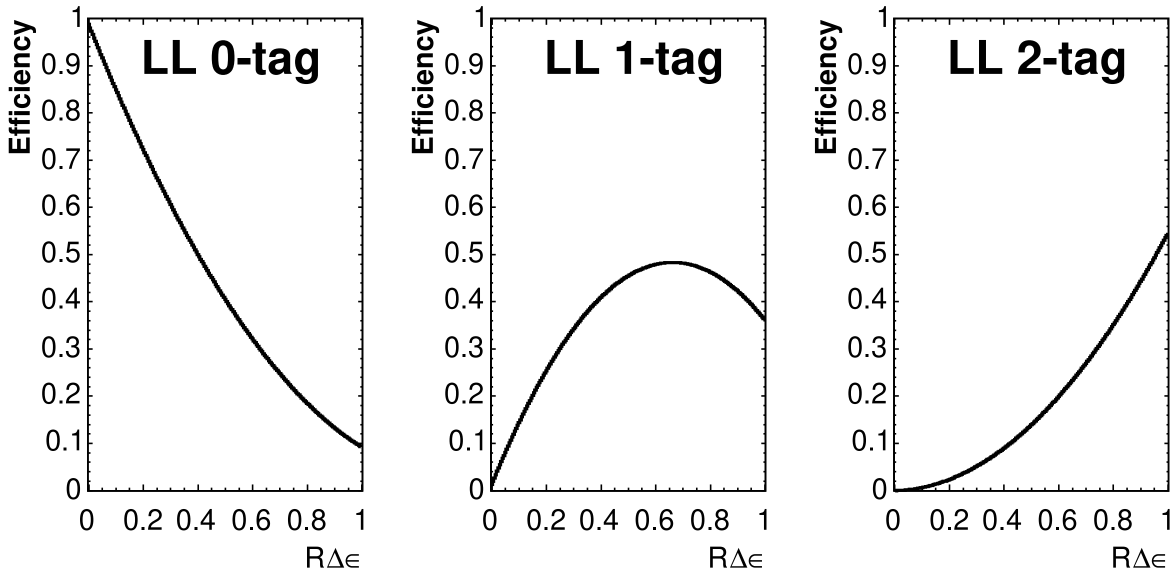

Figure 2: Efficiencies to detect zero (left), one (center) and two (right) tags in dilepton events. The nominal value of $R\Delta\epsilon$ is 0.436.

	L3J	L4J	LL
0-tag	0.497	0.446	0.465
1-tag	0.410	0.428	0.428
2-tag	0.090	0.121	0.107

Table 5: Nominal values of the tagging efficiencies with $\Delta\epsilon = 0.436$.

light-flavor quark and $\Delta\epsilon = \epsilon_b - \epsilon_q$. Thus, we give the event-tagging efficiencies as a function of $R\Delta\epsilon$. For a nominal value of $\Delta\epsilon$ we take 0.436, the average of the values obtained from dilepton and lepton-plus-jets events [5].

Most of the behavior of the efficiency curves is determined by the fraction of the time that zero, one or two b-type jets are within the fiducial region of the silicon detector *i.e.* taggable. This tends to decrease event-tagging efficiencies; if all jets were taggable, the 2-tag efficiency would reach unity. There is a small chance of tagging non-b jets in the event, those that come from W decay or "other" jets that come from QCD radiation. These contributions to the event-tagging efficiency are independent of the value of R. While they are very small, they are non-zero, which is why the 0-tag efficiency never reaches unity and the 1-tag efficiency never reaches zero at $R\Delta\epsilon = 0$. (We note that the Run 1 analysis did not account for these effects [6].) The efficiencies to tag W-decay and "other" jets are computed from simulation and are scaled down by a factor of 0.82 [7]. We take 20% uncertainties on these efficiencies; these will show up in the likelihood, and they are completely correlated across all samples, including both dilepton and lepton-plus-jets. There is no need to take any uncertainty on ϵ_b, when estimating $R\epsilon_b$.

The tag efficiencies assuming the nominal value of $\Delta\epsilon$ are given in Table 5. These values are only used for tests of our sensitivity; they do not always sum to unity because of the possibility of triple-tagging.

3 Likelihood Function

Since we perform the measurement in three independent samples, we can construct three independent likelihood functions, which we multiply together to form the joint likelihood for all samples. The individual likelihoods do have one factor that is correlated – a Gaussian constraint on the efficiency to tag W-decay and "other" jets. This, however, is a small effect.

In general, the likelihood is a product of Poisson probabilities $\mathcal{P}(N_{\mathrm{obs},i}, N_{\mathrm{exp},i})$ that compare the observed number of events with i tags $N_{\mathrm{obs},i}$ with a expected number of events

$$N_{\mathrm{exp},i} = N_{\mathrm{pretag}} \times \epsilon_i + N_{\mathrm{bkgnd},i}. \tag{4}$$

Here, ϵ_i is a function of $R\Delta\epsilon$. N_{pretag} itself a function of ϵ_i, as we will describe below. This means that the presumed N_{pretag} will vary as a function of $R\Delta\epsilon$. In this construction, the likelihood is independent of any assumed value of the total number of $t\bar{t}$ events in the sample, and $R\Delta\epsilon$ is determined only by the relative fractions of events in the sample. The three separate likelihoods differ mostly in how N_{pretag} is estimated, as we now describe.

3.1 Likelihood for L3J

In the L3J sample, we only have information about the $t\bar{t}$ content of the 1-tag and 2-tag samples. Thus

$$N_{\mathrm{pretag}} = \frac{N_{\mathrm{obs},1} + N_{\mathrm{obs},2} - (N_{\mathrm{bkgnd},1} + N_{\mathrm{bkgnd},2})}{\epsilon_1 + \epsilon_2}. \tag{5}$$

While we do not have a real background estimate in the 0-tag sample, we can make use of one piece of information – the background in that sample must be somewhere between 0 and $N_{\mathrm{obs},0}$. Our likelihood function is then

$$\begin{aligned}\mathcal{L} = {} & \mathcal{P}(N_{\mathrm{obs},2}, N_{\mathrm{exp},2})\mathcal{P}(N_{\mathrm{obs},1}, N_{\mathrm{exp},1})(\mathcal{P}(N_{\mathrm{obs},0}, N_{\mathrm{exp},0}) \otimes \mathcal{U}(0, N_{\mathrm{obs},0})) \\ & \otimes \mathcal{G}(\text{bkgnd level}) \otimes \mathcal{G}(\text{bkgnd dist}) \otimes \mathcal{G}(\text{scale factor}).\end{aligned} \tag{6}$$

Here, $\mathcal{U}(0, N_{\mathrm{obs},0})$ represents the constraint that the background in the 0-tag sample is between 0 and $N_{\mathrm{obs},0}$ with uniform probability. This constraint serves as an insurance policy against small $R\Delta\epsilon$. If $R\Delta\epsilon$ were small, then we we would expect a huge number of 0-tag $t\bar{t}$, a number which would never fluctuate down to the $N_{\mathrm{obs},0}$ we observe, even if there were no background in the 0-tag sample.

The $\mathcal{G}$ factors represent Gaussian constraints on the overall background normalization, correlated between the 1-tag and 2-tag samples, on the background distribution, anticorrelated between the 1-tag and 2-tag samples, and the tagging efficiencies, as described above.

3.2 Likelihood for L4J

In this sample, we have much better information about the 0-tag sample from the NN analysis. Now,

$$N_{\mathrm{pretag}} = \frac{N_{\mathrm{obs},0} + N_{\mathrm{obs},1} + N_{\mathrm{obs},2} - (N_{\mathrm{bkgnd},0} + N_{\mathrm{bkgnd},1} + N_{\mathrm{bkgnd},2})}{\epsilon_0 + \epsilon_1 + \epsilon_2}. \tag{7}$$

In fact, while the individual ϵ_i vary with $R\Delta\epsilon$, $\epsilon_0 + \epsilon_1 + \epsilon_2$ is nearly constant for all $R\Delta\epsilon$, and very close to unity at that. As a result, N_{pretag} is nearly constant. Having the 0-tag information provides an important constraint that will improve our uncertainties.

This is illustrated in Figure 3, where we show the progressive sum of the ϵ_i. We can see that the total of the three efficiencies is nearly constant; it only decreases with $R\Delta\epsilon$ because of the increased chances of triple-tagging a $t\bar{t}$ event. This should be contrasted with the curve of $\epsilon_1 + \epsilon_2$, which varies much more rapidly; that curve is the denominator of N_{pretag} in the L3J likelihood. This plot easily illustrates the *fractions* of the total sample that occur as 0-tag, 1-tag and 2-tag events as a function of $R\Delta\epsilon$. Again, it is the fractions that determine $R\Delta\epsilon$. We can see from this plot that the fraction of 1-tag events actually changes very little above $R\Delta\epsilon$ values of about 0.5. Our greatest sensitivity comes from the relative fractions of 0-tag and 2-tag events.

The likelihood for this sample is given as

$$\begin{aligned}\mathcal{L} &= \mathcal{P}(N_{\text{obs},2}, N_{\text{exp},2})\mathcal{P}(N_{\text{obs},1}, N_{\text{exp},1})\mathcal{P}(N_{\text{obs},0}, N_{\text{exp},0}) \\ &\quad \otimes\mathcal{G}(\text{M2 level}) \otimes \mathcal{G}(\text{NN level}) \otimes \mathcal{G}(\text{bkgnd dist}) \otimes \mathcal{G}(\text{scale factor}).\end{aligned} \tag{8}$$

The uncertainties on the overall normalizations of the 0-tag sample (from NN) and the 1-tag and 2-tag samples (from M2) are uncorrelated with each other, and take separate Gaussian constraints. The other constraints are as before.

3.3 Likelihood for LL

As information on all samples is available for dileptons, N_{pretag} is determined in the same way as for the L4J sample. A figure similar to Figure 3 for dileptons has been shown elsewhere [3]. The likelihood function is

$$\begin{aligned}\mathcal{L} = \mathcal{P}(N_{\text{obs},2}, N_{\text{exp},2})\mathcal{P}(N_{\text{obs},1}, N_{\text{exp},1})\mathcal{P}(N_{\text{obs},0}, N_{\text{exp},0}) \\ \otimes\mathcal{G}(\text{bkgnd level}) \otimes \mathcal{G}(\text{bkgnd dist}) \otimes \mathcal{G}(\text{scale factor}).\end{aligned} \tag{9}$$

This is the same as the likelihood for L4J, except that there is only one constraint on background normalizations, and now the uncertainty in the background distribution moves events between the 0-tag and 1-tag samples.

4 Sensitivities

We can test out our likelihood function by determining the precision with which we would measure R and ϵ_b if our the true value of R is one and $\Delta\epsilon = 0.436$, and we were to observe data consistent with these values. That is, we generate 0-tag, 1-tag and 2-tag event counts that are based on the standard-model $t\bar{t}$ cross section of 6.7 pb with $R = 1$, the known detection efficiency for detecting such events after making the dilepton [8] and lepton-plus-jets [9] selections, and the tagging efficiencies and backgrounds described in Section 2.

In the 161 pb^{-1} data sample we expect 36.5 L3J events, 44.7 L4J events and 6.5 LL events from $t\bar{t}$ before tagging. These values are multiplied by the nominal tagging efficiencies of Table 5 to obtain the number of $t\bar{t}$ signal events in our 3×3 subsamples. We sum these with the background estimates of Tables 2, 3 and 4, to obtain the N_{obs} that we use as N_{obs} in our likelihood function, as shown in Table 6. (The 0-tag background in L3J is chosen so that the total number of events in the sample (358) is what we observe in the data.)

Figure 4 shows the resulting likelihood distributions from the three separate samples, and the product (combined likelihood). All of them peak at $R\Delta\epsilon = 0.436$, the nominal value when $R = 1$ and $\Delta\epsilon = 0.436$; this tells us that our likelihood function is correct, at least at the level that we can get out of it what we put into it. The widths of these distributions indicate the sensitivity of the different samples to $R\Delta\epsilon$. Most of our sensitivity comes from the L4J sample; the L3J contributes very little. The LL sample also has little sensitivity, but we will want to see consistency between lepton-plus-jets and dilepton events.

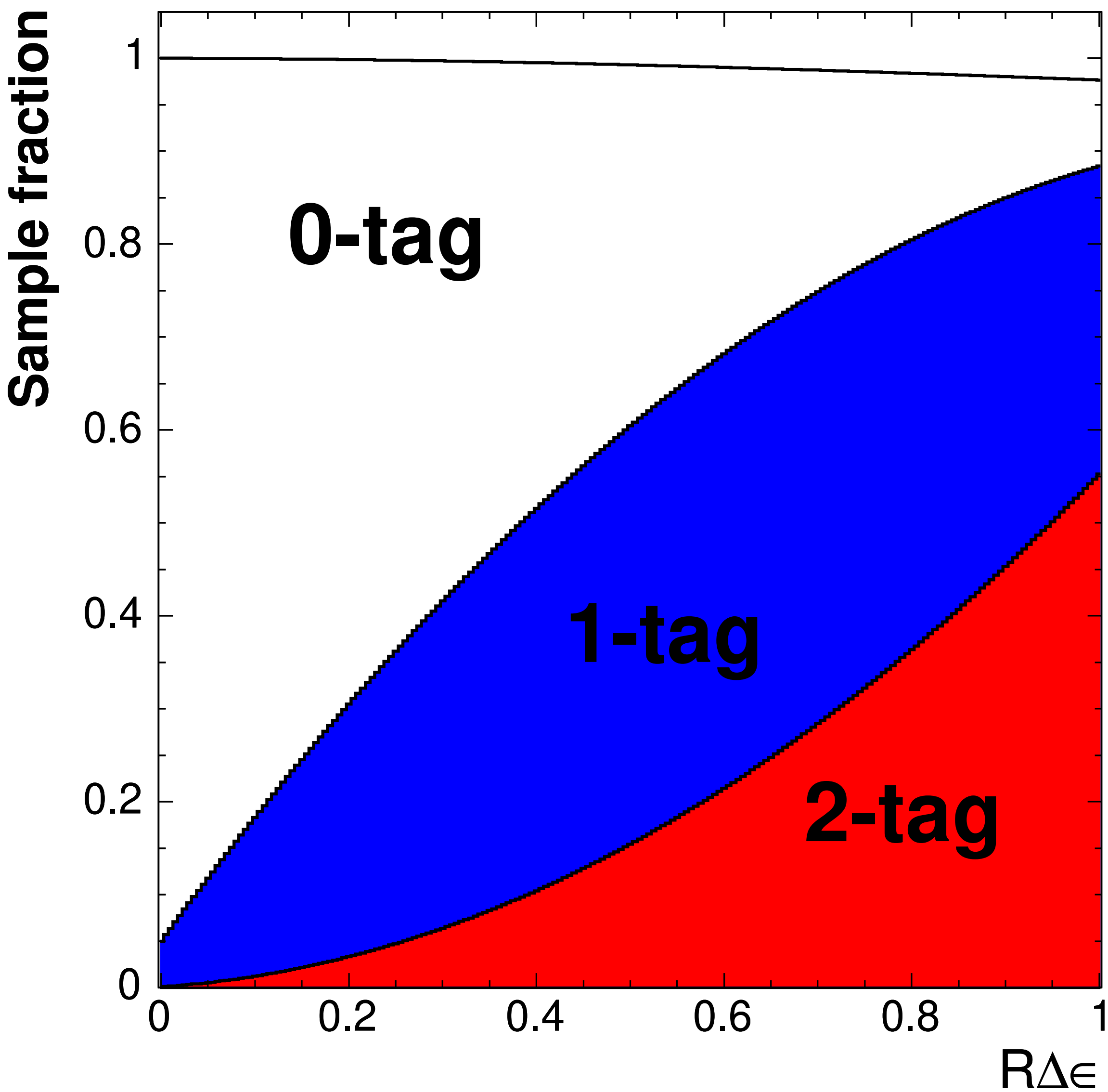

Figure 3: $t\bar{t}$ sample fractions as a function of $R\Delta\epsilon$. The red curve is the efficiency to observe two tags, and the red region indicates the fraction of 2-tag events in the sample. The blue and white regions are defined similarly for 1-tag and 0-tag events. The black line at nearly unity is the total efficiency. The nominal value of $\Delta\epsilon$ is 0.436.

Sample	L3J	L4J	LL
0-tag	18.2 + 339.8 = 358.0	19.9 + 62.3 = 82.2	3.0 + 2.0 = 5.0
1-tag	15.0 + 16.0 = 21.0	19.1 + 4.2 = 23.3	2.8 + 0.2 = 3.0
2-tag	3.3 + 0.8 = 4.1	5.4 + 0.2 = 5.6	0.7 + 0.0 = 0.7

Table 6: Signal plus background counts in the sensitivity test.

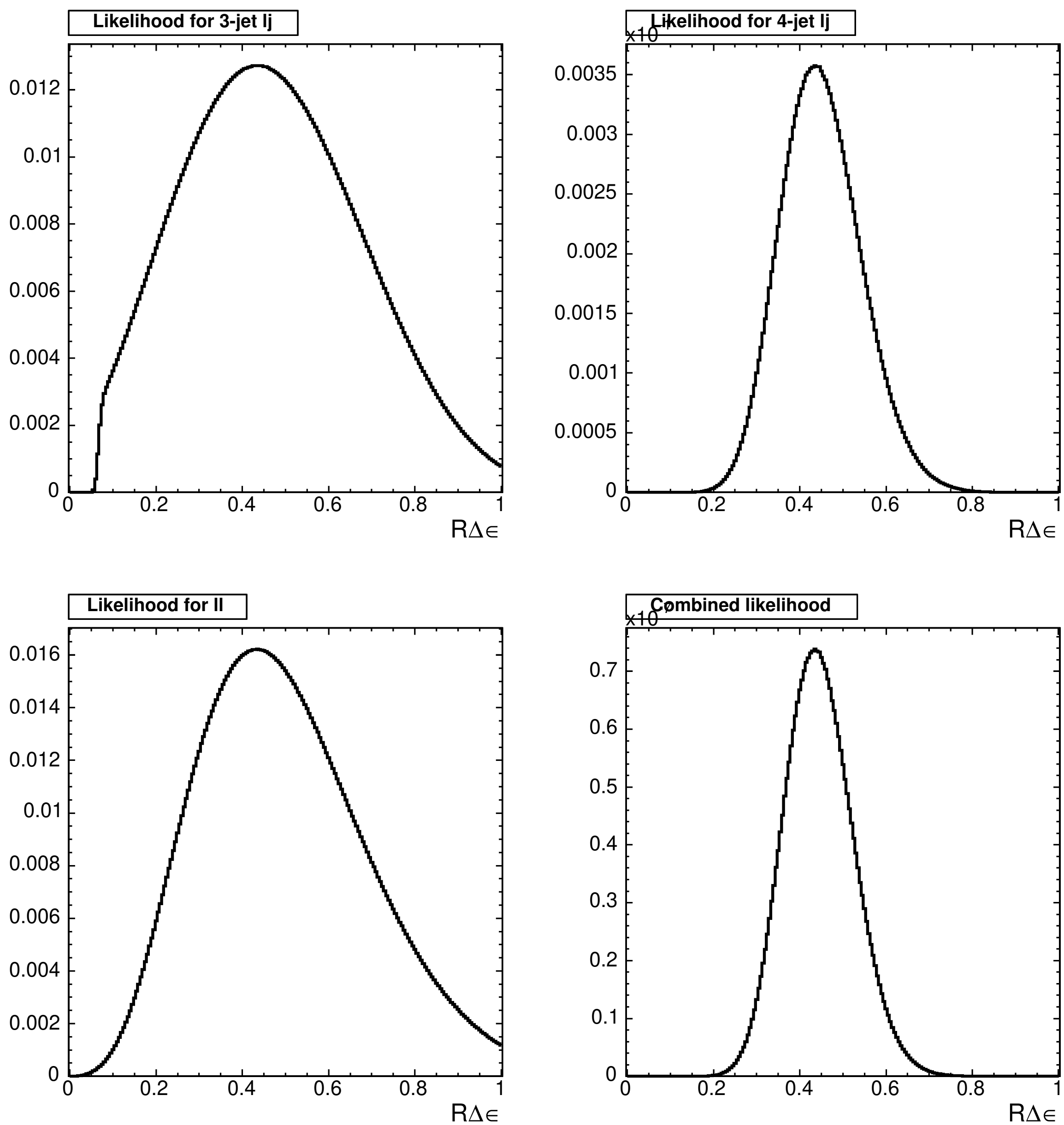

Figure 4: Likelihoods as a function of $R\Delta\epsilon$ for the dilepton sample in the sensitivity test: L3J (top left), L4J (top right), LL (bottom left) and combined (bottom right).

Sample	Central value	Lower limit
L+J	$0.44^{+0.09}_{-0.08}$	0.31
LL	$0.44^{+0.21}_{-0.17}$	0.21
All	0.44 ± 0.08	0.32

Table 7: Results for $R\Delta\epsilon$ from the sensitivity test.

There are two basic numerical results that we obtain from the likelihood, which lead to a few further results after some simple manipulation. The first is the central value of $R\Delta\epsilon$ and its uncertainty. For this, we quote the value of $R\Delta\epsilon$ that maximizes the likelihood function, and the boundaries of the highest probability density interval, which is the shortest interval containing 68.3% of the likelihood area. The second is the 95% CL lower limit on $R\Delta\epsilon$. For this, we take the approach of assuming that $R\Delta\epsilon$ must fall in the physical range between zero and one. We integrate the likelihood function from $R\Delta\epsilon = 0$ up to a value of $R\Delta\epsilon$ such that 5% of the total area of the likelihood is contained in the integral. From this central value and lower limit, we can estimate R using our known value of $\Delta\epsilon$, or determine ϵ_b using $R = 1$ and ϵ_q. The results of the sensitivity test are given in Table 7. For the combined analysis, we expect a precision of 18% on $R\Delta\epsilon$.

The systematic uncertainties are very small compared to the statistical uncertainties, sufficiently small that if we set the widths of the constraining Gaussians to zero in the likelihood, we obtain the same result for $R\Delta\epsilon$ in the sensitivity test, with the same uncertainties. This can be seen in Figure 5, which shows the likelihood functions obtained with the constraining Gaussians at their nominal widths, and with width zero. We only compute the likelihood for discrete values of $R\Delta\epsilon$ in steps of 0.005. This resolution is entirely reasonable considering the precision of the measurement, but is coarse enough to obscure the contribution of the small systematic uncertainties. However, we can get a rough estimate of the size of these uncertainties by just comparing the RMS width of the likelihood distributions with and without the systematic uncertainties accounted for. With systematics, the width is 0.0827, and without it is 0.0781, implying a systematic uncertainty of 0.027 on $R\Delta\epsilon$, or about 6.2% (relative) on the result. This uncertainty is therefore lost in the larger statistical uncertainty. This systematic uncertainty does not include uncertainties on $\Delta\epsilon$ itself, which must be accounted for when we extract a value of R. We note that uncertainties that are correlated across samples with different numbers of tags have a very small impact on the precision, as they tend not to affect the tag ratios too much. Effects that move events between tag samples would have a larger impact, but those uncertainties are tiny. The relatively large systematic uncertainty on the L4J 0-tag background leads to the largest systematic uncertainty on the final result; in the analysis that only uses the Method 2 backgrounds, the systematic uncertainty is only 3.0% [1]. But even that background uncertainty is small, and is well worth taking on for the constraint that that sample provides.

These are the results we would obtain if we observed exactly the event counts derived from the predicted values. Of course, there will be statistical fluctuations in the observed production rates for $t\bar{t}$ and the backgrounds. To estimate the range of results we might get, we throw pseudo-experiments based on the central values quoted above. To save time, we neglect the small systematic uncertainties in both the generation of the experiments, and in evaluating the likelihood. In each pseudo-experiment, we draw random numbers for the number of $t\bar{t}$ events before tagging from a Poisson distribution, and decide how many tags each event has using random numbers and the tagging efficiencies of Table 5. We also draw random numbers for the background levels from Poisson distributions with means given in Tables 2, 3 and 4, and widths based background uncertainties. These numbers are used to create new event counts which are used as N_{obs} in the likelihood function,

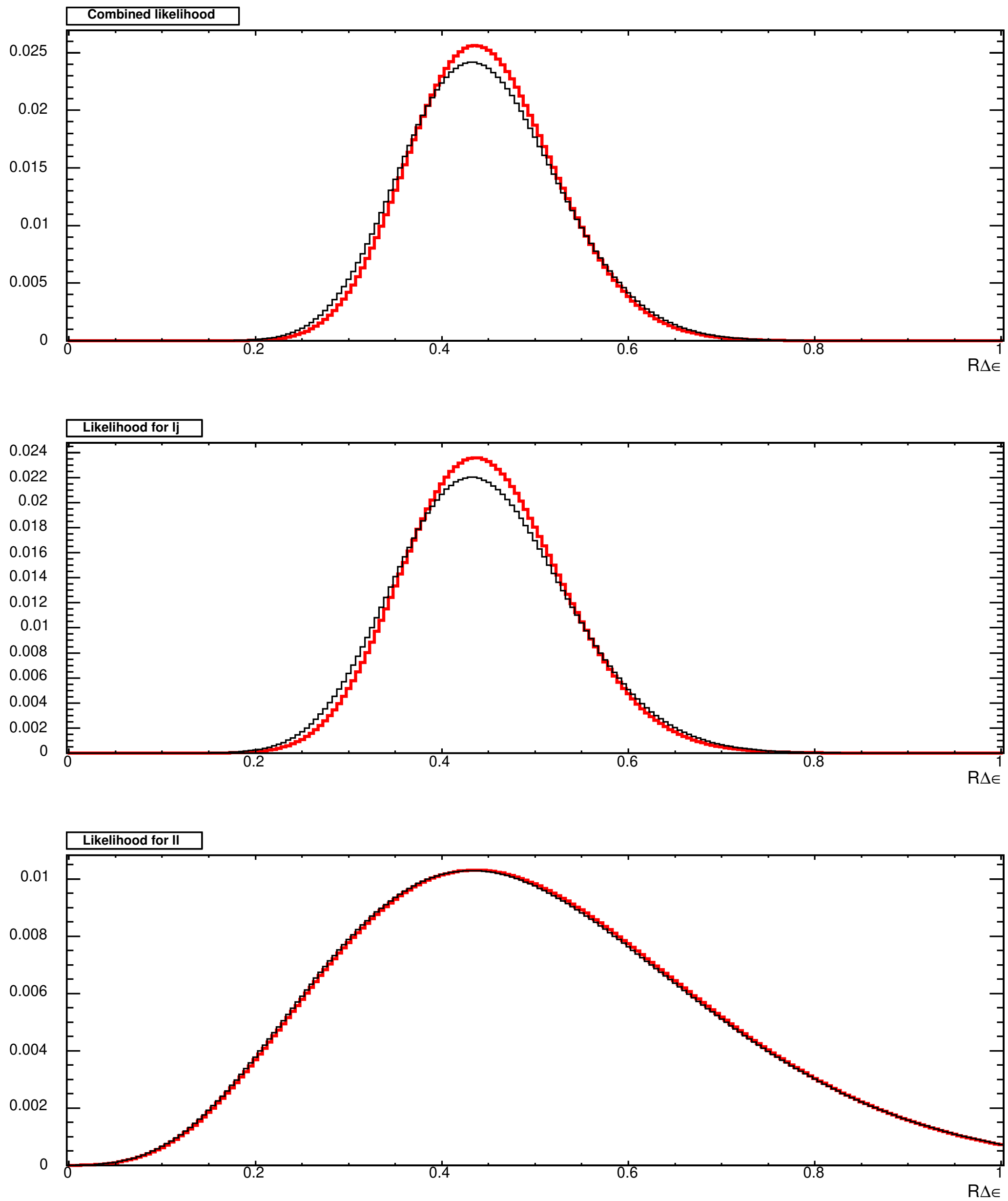

Figure 5: Comparison of likelihood functions when systematic uncertainties are included (black) and when they are not (red) for the combined (top), L+J (middle) and LL (bottom) samples. The pairs of curves are normalized to equal area.

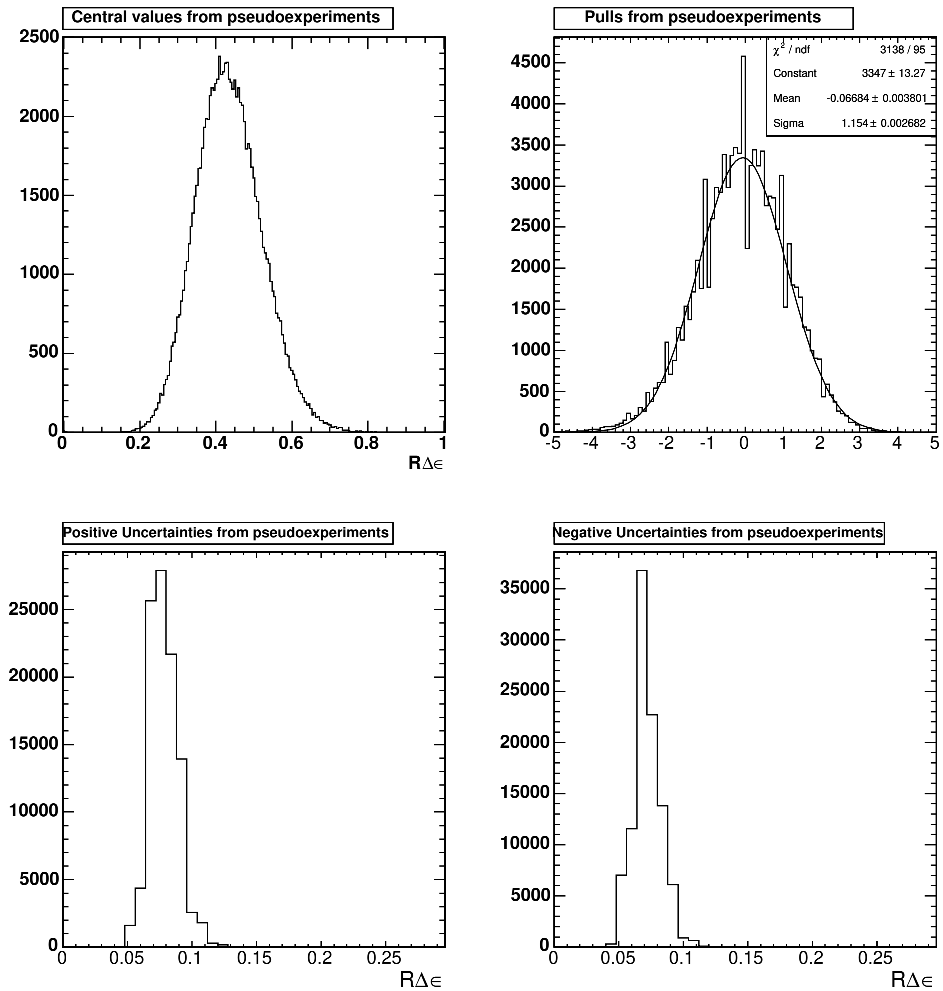

Figure 6: Distribution of central values (upper left), pulls (upper right), positive-side uncertainties (lower left) and negative-side uncertianties (lower right) for $R\Delta\epsilon$ from 100000 pseudo-experiments.

and we extract the central value, uncertainty and lower limit for each experiment.

The results of 100000 pseudo-experiments are shown in Figure 6. The pull distribution is close to Gaussian and has a width slightly larger than one. If $\sigma_{t\bar{t}} = 6.7$ pb and $R = 1$, and if we have estimated our efficiencies and backgrounds correctly, we expect typical uncertainties of 0.05 to 0.10 on $R\Delta\epsilon$.

5 Results and Conclusions

Finally, we examine the lepton-plus-jets and dilepton events in the data. Table 8 gives the distribution of tag counts for the three different events in the 161 pb^{-1} of collision data. After subtracting backgrounds, we can get rough estimates of $R\Delta\epsilon$ by just taking ratios of tag rates. For instance, in the L3J sample, we observe a single- to double-tag ratio of 4.54 when we expect 4.56. In the L4J sample, the ratios of 0-tag, 1-tag and 2-tag $t\bar{t}$ events are 0.414:0.467:0.119, when we expect 0.446:0.428:0.121, which implies a larger-than-expected $R\Delta\epsilon$. In the dileptons, the observed ratios

Sample	L3J	L4J	LL
0-tag	358	79	5
1-tag	26	23	4
2-tag	3	5	2

Table 8: Event counts in the 161 pb^{-1} of collision data.

Sample	Central value	Lower limit
L+J	$0.46^{+0.10}_{-0.09}$	0.32
LL	$0.61^{+0.19}_{-0.16}$	0.36
All	$0.49^{+0.09}_{-0.08}$	0.37

Table 9: Results for $R\Delta\epsilon$ from the data.

are 0.326:0.442:0.232, which can be compared to the expected values of 0.465:0.428:0.107; we observe more (twice as many) double-tagged events, and fewer untagged events, than we had expected, also implying a larger $R\Delta\epsilon$.

Figure 7 show the likelihood distributions, which can be compared with Figure 4, and Figure 8 repeats the final product likelihood for display purposes. The results for the different samples are given in Table 9. We find $R\Delta\epsilon = 0.49^{+0.09}_{-0.08}$, and $R\Delta\epsilon > 0.36$ at 95% CL.

The central value is consistent with the expected value of 0.436. If we assume $\Delta\epsilon = 0.436 \pm 0.032$, and naively divide, then we estimate $R = 1.11^{+0.21}_{-0.19}$. Alternatively, if we assume $R = 1$, then $\epsilon_b = 0.49^{+0.09}_{-0.08}$, when we expect 0.436. Our uncertainties are within the range expected from pseudo-experiments.

In order to make sure that our final result is physically allowed, we implement the framework advocated by Feldman and Cousins [12, 2]. To start, we throw ensembles of pseudo-experiments for different values of R_{true} and fit the resulting R_{measured} distributions. Using these fits and the F-C likelihood-ratio ordering principle, we construct 68.3% and 95% acceptance bands. After finding the smallest R_{true} for which our measured value of R is within the 95% acceptance band, we use this value as our lower limit.

This technique naturally handles issues such as biases and non-unit pulls. We also handle systematic uncertainties by making variations in the pseudo-experiments. Before drawing random numbers for the event counts from Poisson distributions, we smear the means for these distributions by the appropriate uncertainties. When choosing the number of $t\bar{t}$ events before tagging, we smear the mean by the uncertainty on the acceptance and luminosity. When deciding how many of the $t\bar{t}$ events have tags, we vary the single-jet tagging efficiencies according to their uncertainties and recalculate the event-tagging efficiencies. Some portions of the background estimates that come from Method 2 (those which depend on the simulation, *i.e.* everything except for mistags and QCD [13]) are correlated with these tagging efficiencies, and we vary those parts in a correlated fashion. That is, if the efficiency to tag $t\bar{t}$ events increases, the amount of backround in the L3J and L4J 1-tag and 2-tag samples also increases. The backgrounds affected by this are about half of the 1-tag background, and the entire 2-tag background. All remaining backgrounds, including those for the dilepton sample and from the neural-net analysis, are smeared independently according to their uncertainties. These smeared background estimates are then used as means for Poisson distributions used to generate the background counts in the pseudo-experiments.

Figure 9 compares the results of pseudo-experiments thrown taking systematic uncertainties

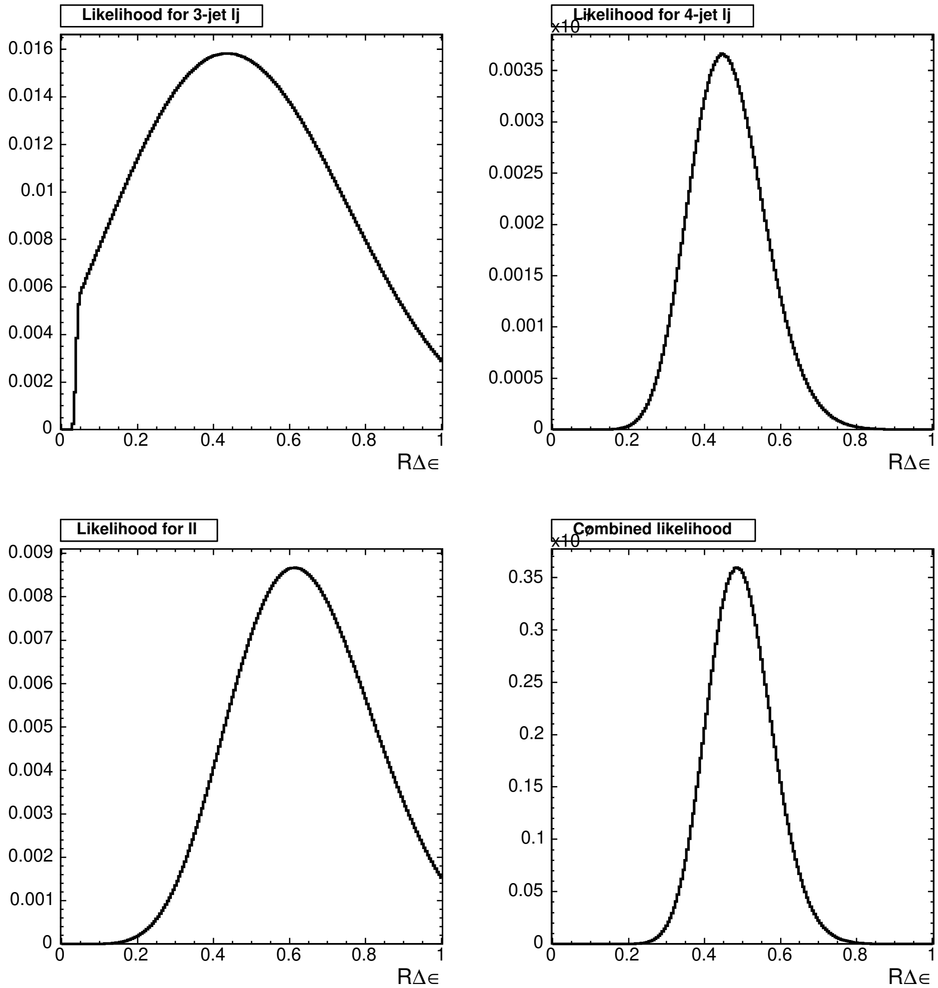

Figure 7: Likelihoods as a function of $R\Delta\epsilon$ for the three data samples.

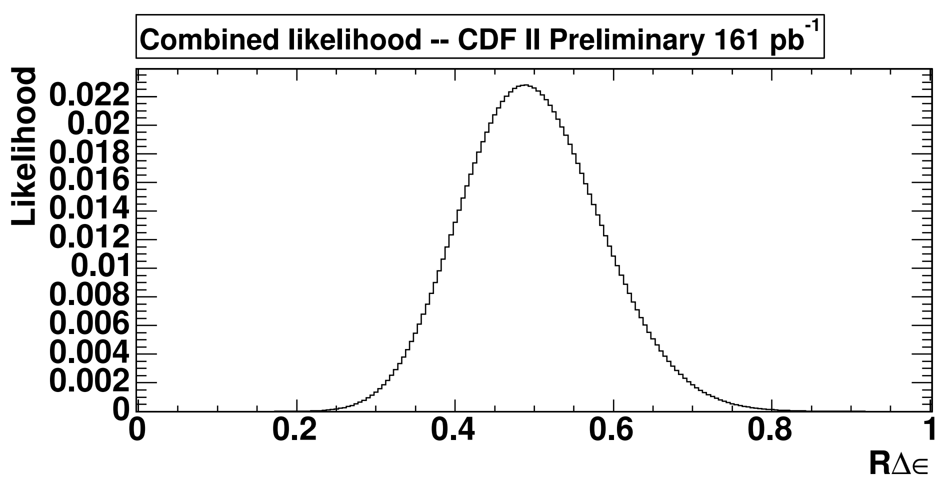

Figure 8: Combined likelihood for all three data samples as a function of $R\Delta\epsilon$.

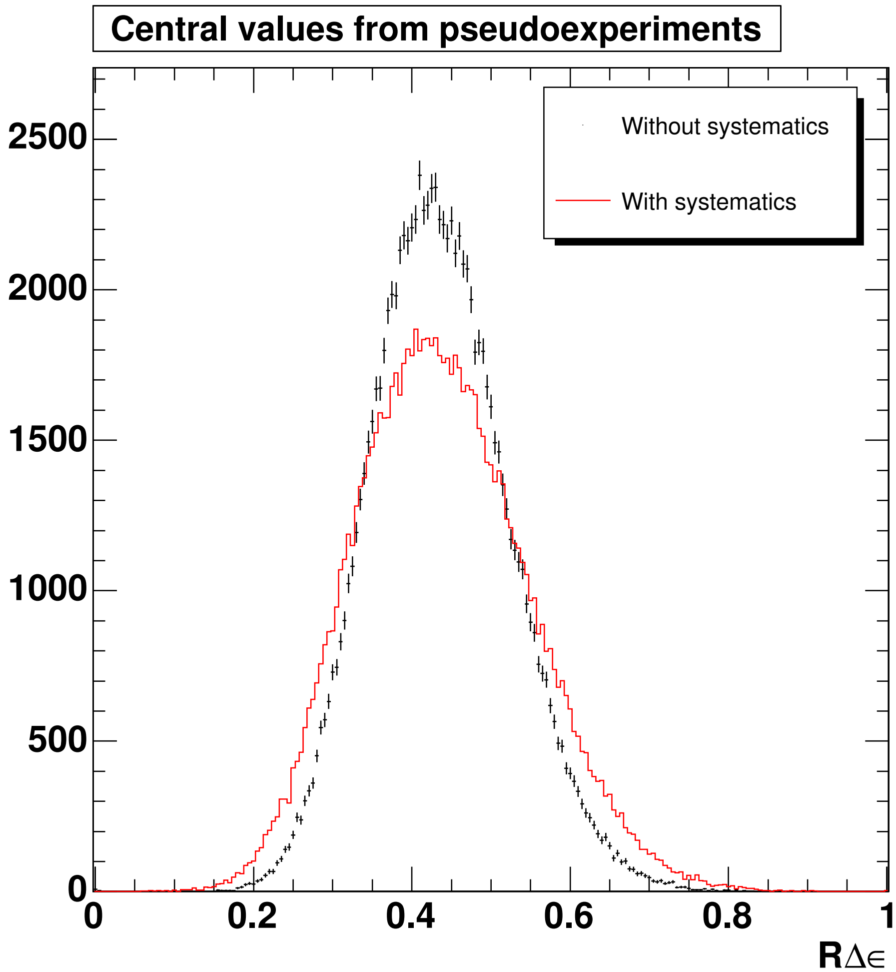

Figure 9: Distributions most-likely values from pseudo-experiments thrown assuming $R_{\rm true} = 1$, both with (red) and without (black) accounting for systematic uncertainties.

into account to the results of pseudo-experiments that ignore the uncertainties. We can see a clear broadening of the distribution once systematics are accounted for. Note that we have now incorporated the systematic uncertainty on the b-tagging efficiency into the smearing, unlike the example in Section 4. That uncertainty is 7.3%; with other uncertainties affecting the measurement of $R\Delta\epsilon$ at the 6.1% level, the b-tagging efficiency contributes the largest single uncertainty to the extraction of R.

Figure 9 is made for $R_{\rm true} = 1$. We make similar distributions for different values of $R_{\rm true}$, and for each we estimate confidence intervales. These are shown in Figures 10 (which does not include systematic uncertainties) and 11 (which does). Given our measured value of $R = 1.11$, we set a 95% CL lower limit on R of 0.70 when systematics are ignored, and 0.62 when they are included.

Our results are consistent with the expectation from the standard model. More importantly, we have made a measurement of R with an uncertainty of about 20%, easily exceeding the precision of the Run 1 measurement [6], which found $R = 0.94^{+0.31}_{-0.24}$ and $R > 0.56$ at 95% CL. We expect to publish our results soon.

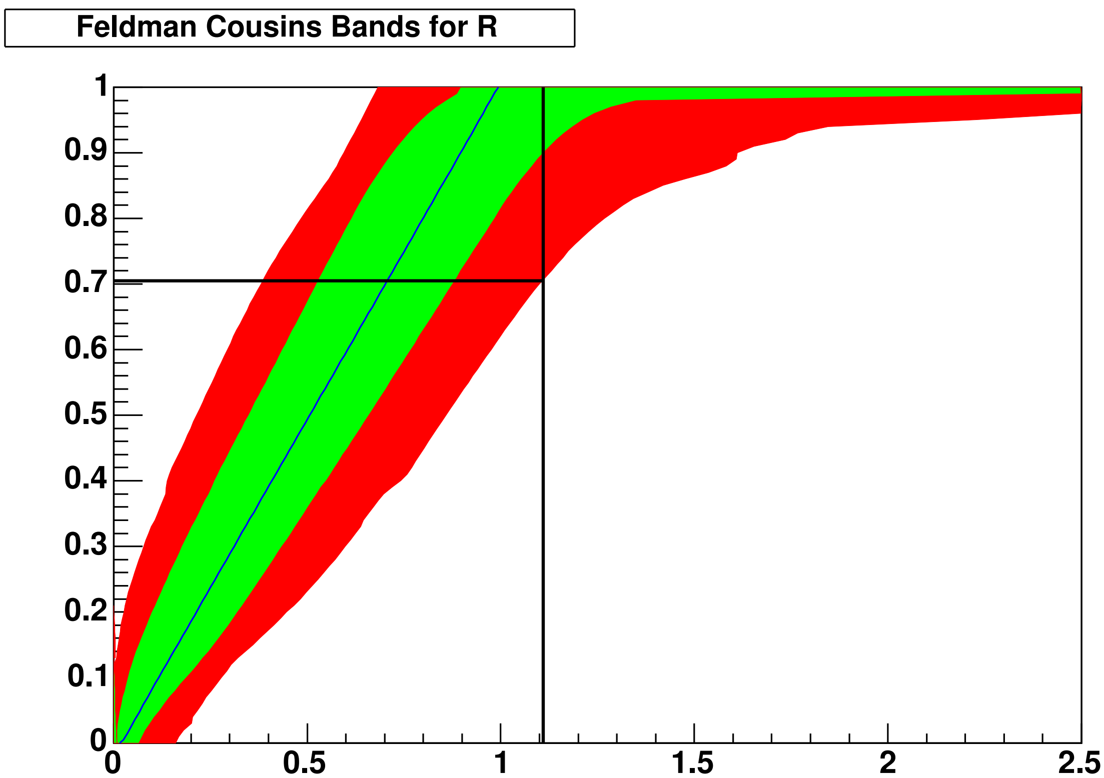

Figure 10: Feldman-Cousins 68.3% (green) and 95% (red) confidence bands *vs.* measured R, accounting for statistical uncertainties only. With our measurement of $R = 1.11$, the lower limit is 0.70.

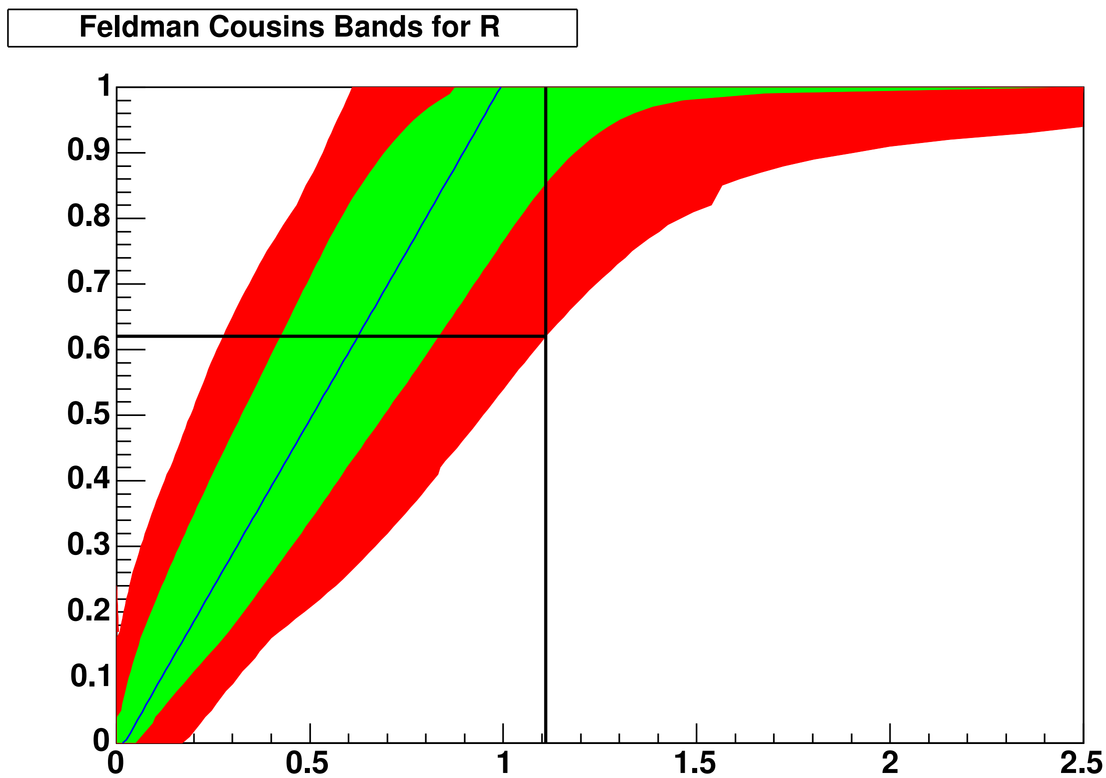

Figure 11: Feldman-Cousins 68.3% (green) and 95% (red) confidence bands *vs.* measured R, accounting for both statistical and systematic uncertainties. With our measurement of $R = 1.11$, the lower limit is 0.62.

References

[1] K. Bloom *et al.*, CDF 7012.

[2] M. Gold *et al.*, CDF 7067.

[3] K. Bloom and M. Tecchio, CDF 7100.

[4] K. Bloom *et al.*, CDF 6822.

[5] K. Bloom *et al.*, CDF 7070.

[6] T. Affolder *et al.*, PRL **86**, 3233 (2001).

[7] H. Bachacou *et al.*, CDF 6904.

[8] D. Goldstein *et al.*, CDF 6830.

[9] K. Bloom *et al.*, CDF 6822.

[10] D. Acosta *et al.*, CDF 6882, submitted to PRL.

[11] A. Dominguez *et al.*, CDF 6533.

[12] G. Feldman and R. Cousins, PRD **57**, 3873 (1998).

[13] J.S. Miller and D. Amidei, CDF 6907.